JOURNAL OF THE ROYAL SOCIETY Interface

Characterization and use of laser-based lysis for cell analysis on-chip

Hsuan-Hong Lai, Pedro A Quinto-Su, Christopher E Sims, Mark Bachman, G.P Li, Vasan Venugopalan and Nancy L Allbritton

J. R. Soc. Interface 2008 **5**, S113-S121
doi: 10.1098/rsif.2008.0177.focus

Interface focus

J. R. Soc. Interface (2008) **5**, S113–S121
doi:10.1098/rsif.2008.0177.focus
Published online 26 June 2008

Characterization and use of laser-based lysis for cell analysis on-chip

Hsuan-Hong Lai[1,3], Pedro A. Quinto-Su[2], Christopher E. Sims[3], Mark Bachman[1], G. P. Li[1], Vasan Venugopalan[2] and Nancy L. Allbritton[3,*]

[1]*Department of Electrical Engineering and Computer Science, and* [2]*Department of Chemical Engineering and Materials Science, University of California, Irvine, CA 92697, USA*
[3]*Department of Chemistry, University of North Carolina, Chapel Hill, NC 27599, USA*

We demonstrate the use of a pulsed laser microbeam for cell lysis followed by electrophoretic separation of cellular analytes in a microfluidic device. The influence of pulse energy and laser focal point within the microchannel on the threshold for plasma formation was measured. The thickness of the poly(dimethylsiloxane) (PDMS) layer through which the beam travelled was a critical determinant of the threshold energy. An effective optical path length, L_{eff}, for the laser beam can be used to predict the threshold for optical breakdown at different microchannel locations. A key benefit of laser-based cell lysis is the very limited zone (less than 5 μm) of lysis. A second asset is the rapid cell lysis times (approx. microseconds). These features enable two analytes, fluorescein and Oregon Green, from a cell to be electrophoretically separated in the channel in which cell lysis occurred. The resolution and efficiency of the separation of the cellular analytes are similar to those of standards demonstrating the feasibility of using a pulsed laser microbeam in single-cell analysis.

Keywords: chemical cytometry; laser microbeam; electrophoresis; poly(dimethylsiloxane); microchannel

1. INTRODUCTION

Chemical analysis techniques for single-cell studies, an area commonly referred to as chemical cytometry, are in a phase of rapid development (Dovichi & Hu 2003). An area of particularly intense research in the analytical community is the implementation of microfluidic devices for the electrophoretic separation of analytes derived from single cells (Di Carlo & Lee 2006; Price & Culbertson 2007; Sims & Allbritton 2007). The very small volume of most cells (approx. 1 pl) and nano- to micromolar concentrations of biological compounds mandate highly sensitive detection schemes, typically by laser-induced fluorescence (LIF) (Paez & Hernandez 2001; Zhang *et al.* 2002; Lin *et al.* 2003; Lacroix *et al.* 2005). On-chip electrophoretic analyses of single cells have included a variety of different analytes including fluorescently labelled amino acids, esterified dyes, reactive oxygen species, glutathione, DNA and proteins (Waters *et al.* 1998; McClain *et al.* 2003; Gao *et al.* 2004; Munce *et al.* 2004; Woods *et al.* 2004; Wu *et al.* 2004; Hellmich *et al.* 2005,2006; Wood *et al.* 2005; Martin *et al.* 2006; Ros *et al.* 2006; Huang *et al.* 2007). A number of investigators have addressed the microfluidic-based manipulation of cells and cellular contents that often must occur prior to electrophoretic analysis. These operations include cell transport (Li & Harrison 1997), cell sorting (Wang *et al.* 2007), cell entrapment (Braschler *et al.* 2005; Johann 2006; Evander *et al.* 2007), cell encapsulation (Tan *et al.* 2006) and cell lysis (He *et al.* 2005; Lu *et al.* 2005), among others. The lab-on-chip format has the potential to increase throughput and reduce the personnel required to conduct these analyses by automating cell movement and buffer exchange, decreasing analyte separation times and implementing parallel and serial analyses of cells.

Cell lysis becomes an important issue for accomplishing the separation of analytes derived from individual cells. Cellular contents must be released into the separation channel rapidly and controllably to prevent sample loss; furthermore, the time required for disruption of cellular membranes establishes the temporal resolution of the measurement (Sims *et al.* 1998). Chemical and electrical lysis of cells have been successfully mated with electrophoretic analysis of the contents of single cells on-chip (Di Carlo & Lee 2006; Price & Culbertson 2007; Sims & Allbritton 2007). Chemical disruption of the plasma membrane of a mammalian cell typically requires many seconds (Kleparnik & Horky 2003; Gao *et al.* 2004; Wu *et al.* 2004). This approach is simple to implement in a microfluidic device, and is suitable when evaluating cellular analytes whose concentrations are static, change slowly or are not affected by the lysis procedure (e.g. nucleotides and most proteins). When the goal is to measure the state of cellular analytes that are altered on second to subsecond time scales, e.g. second messenger concentrations, protein phosphorylation and dephosphorylation, more rapid

*Author for correspondence (nlallbri@unc.edu).

One contribution of 7 to a Theme Supplement 'Single-cell analysis'.

Received 1 May 2008
Accepted 10 June 2008

cell lysis is desirable (Meredith *et al.* 2000; Li *et al.* 2001). Subsecond cell lysis has been achieved in microfluidic devices by pairing electrical with chemical lysis (McClain *et al.* 2003) and by laser-mediated membrane disruption (He *et al.* 2005; Quinto-Su *et al.* 2008). These approaches are easily implemented, but do require integration of electrodes or focusing of a pulsed laser in the microchannel.

Although rapid cell lysis using a laser has been demonstrated in a microfluidic device, its combination with electrophoretic analysis has yet to be performed. Nonetheless, disruption of the cell's plasma membrane within a microfluidic channel using a pulsed pico- to nanosecond laser can be expected to have a number of advantages for on-chip chemical cytometry. Provided the device is optically transparent, the laser can be easily integrated at any position in the device in order to target a specific cell or location for lysis. The photoinduced lysis process is confined to a small area so that individual cells can be lysed without disrupting nearby cells (Quinto-Su *et al.* 2008). The laser can also be used to disrupt a portion of the membrane by positioning a microbeam in a subcellular region (Li *et al.* 2001), or the entire cell can be lysed using a focused pulse to generate a plasma and cavitation bubble that mechanically disrupts the membrane (Rau *et al.* 2004, 2006). Furthermore, laser-based cell lysis is known to occur on microsecond time scales, which is desirable for the study of many biochemical reactions that may fluctuate over milliseconds (Berridge 1993; Sims *et al.* 1998; Rau *et al.* 2006). In a prior study, time-resolved imaging was used to study laser-based cell lysis in a microchannel (Quinto-Su *et al.* 2008). A hybrid device composed of a poly(dimethylsiloxane) (PDMS) channel on a glass substrate was used for optimal laser focusing and in-channel imaging. Using a fixed laser focal point (2 μm above the glass channel bottom) and constant pulse energy (twofold that required to generate a plasma), cell lysis was shown to occur on the nano- to microsecond time scale. Interestingly, the cellular contents were dispersed by the expansion of the laser-induced cavitation bubble, but bubble collapse relocalized cellular contents to a small region without extensive dilution. These findings suggested that optimization of the in-channel laser-based lysis would be valuable for on-chip chemical cytometry applications.

In the current study, a detailed examination was performed to establish the optimal parameters for laser-based single-cell lysis in a PDMS separation channel. The pulse energy of the laser, the position of the laser focal point relative to the cell and its position relative to the floor of the microchannel were varied and correlated with cell lysis. In order to provide a suitable micro-column for electrophoresis, the microfluidic device was manufactured so that all four walls of the cell lysis region and the separation channel were composed of PDMS. The influence of the PDMS base layer on the laser microbeam was evaluated by varying the layer's thickness and evaluating the threshold for plasma formation within the channel. Lastly, the fluorescent cytosolic contents released from a single cell lysed in the channel were electrophoretically separated to demonstrate the feasibility of chemical cytometry employing laser-based lysis on-chip.

2. EXPERIMENTAL SECTION

2.1. Reagents

PDMS (SYLGARD 184) was purchased from Dow Corning (Midland, MI). RPMI 1640 (with L-glutamine and HEPES), foetal bovine serum, penicillin and streptomycin were obtained from Invitrogen (Carlsbad, CA). Fluorescein diacetate, fluorescein-free acid (fluorescein), Oregon Green 488 carboxylic acid diacetate (Oregon Green diacetate) and Oregon Green 488 carboxylic acid (Oregon Green) were purchased from Molecular Probes (Eugene, OR). The perfluoroalkyl silane, (heptadecafluoro-1,1,2,2-tetrahydrodecyl)trichlorosilane, was obtained from Gelest Inc. (Morrisville, PA). All other reagents were purchased from Sigma-Aldrich (St Louis, MO).

2.2. Cell culture

BA/F3 cells (mouse leukaemia) were cultured and loaded with fluorescent analytes (Oregon Green diacetate and/or fluorescein diacetate), as described previously (Sims *et al.* 1998). Just prior to use in the microchips, the cells were exchanged into either a physiological extracellular buffer (ECB) or an isotonic, low-salt buffer (1 mM KH_2PO_4, 4 mM Na_2HPO_4, 245 mM D-mannitol and 40 mM poly(ethylene glycol) (MW 1000, PEG1K; pH 7.4)). The composition of the isotonic buffer was chosen to mimic the osmolarity of physiological ECB without using high salt concentrations and was used only for electrophoresis of cell contents.

2.3. Fabrication of microfluidic devices

All microfluidic devices were composed of two parts. The top portion of the microfluidic device was made of PDMS moulded on a silicon master fabricated as described previously (Ren *et al.* 2001). Prior to the first use, the silicon master was silanized using a vapour phase reaction with the hydrophobic reagent (heptadecafluoro-1,1,2,2-tetrahydrodecyl)trichlorosilane (Wang *et al.* 2006). The surface silanization was carried out to facilitate lift-off of the cast PDMS microstructure from the silicon master. The channels imprinted into the PDMS were 50 μm wide and 50 μm deep. Access ports or holes were also punched into the 1 mm thick top piece at the ends of the imprinted channels. The bottom portion of the microfluidic device (bottom piece) was a PDMS-coated cover glass. The upper and lower pieces of the device were sealed together by pressure and wells (2 mm high plastic tubing, 0.64 cm outside diameter and 0.43 cm internal diameter) were epoxied onto the channel-access holes to form liquid reservoirs.

The thickness of the PDMS composing the bottom piece of the device (L_{PDMS}) was carefully controlled during fabrication. To fabricate the bottom piece, SYLGARD 184 pre-polymer mixture was spin coated onto a cover glass (Goldseal Cover Glass, No. 0 thickness, 24 mm×60 mm; Ted Pella, Inc., Redding, CA). The cover glass with the PDMS pre-polymer was spun (WS-400B-6NPP-LITE spin processor; Laurell Technologies Corp., North Wales, PA) at 500*g* for 10 s

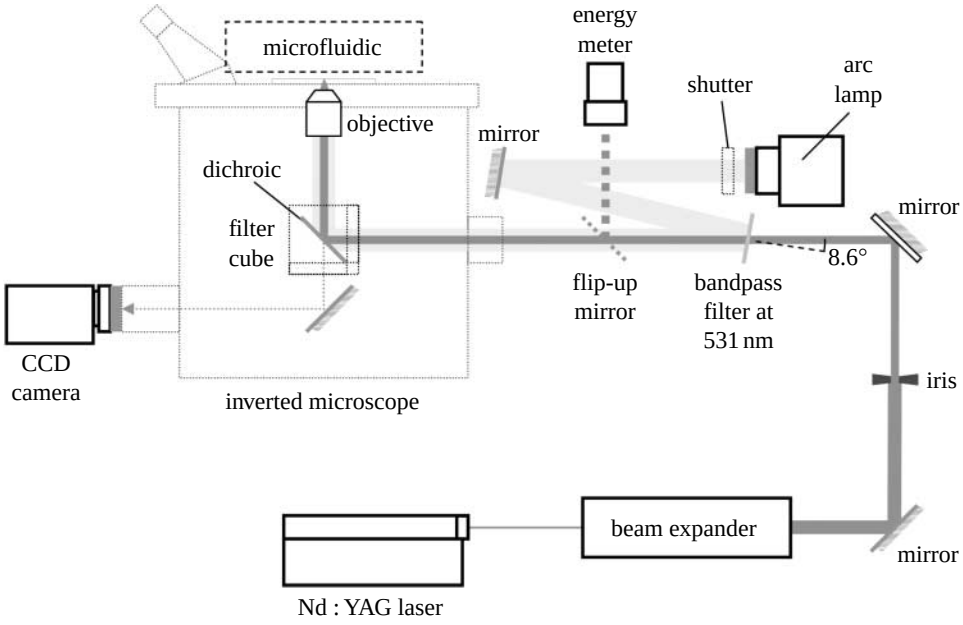

Figure 1. Schematic of the optical delivery system for the laser beam.

followed by a second spin for 50 s at 1400–1800*g* depending on the desired film thickness. After coating, the cover glass with the PDMS film was baked on a thermoplate at 95°C for 10 min. The thickness of the PDMS film on the cover glass was determined by measuring the thickness of the cover glass before and after the PDMS coating using a micrometer (Fowler 74-860-001 electronic micrometer, 0.001 mm resolution; Fred V. Fowler Co., Newton, MA).

For the microchips used for electrophoresis, the thickness of the top piece was 150–350 µm. The PDMS pre-polymer was spin coated (400*g*, 1 min) onto a silicon master. The silicon master with the spin-coated PDMS layer was then placed in the vacuum desiccator (7 Torr) to degas. To avoid cracking of the silicon master, the vacuum was slowly released. To vulcanize the thin PDMS layer, the coated silicon master was transferred onto a thermoplate to bake at 95°C for 10 min. After cooling to room temperature, the thickness of the PDMS plus silicon master was measured and compared with that of the silicon master prior to coating to determine the thickness of the PDMS film. The PDMS film was then peeled off from the silicon master. Channel-access holes (approx. 1 mm in diameter) were then punched through at the four termini of the simple cross-channel geometry. The top piece was then polymer grafted as described below and mated to a grafted bottom piece by pressing them together.

2.4. Polymer grafting of the PDMS microchannels

The top and bottom pieces of the microchannels used for electrophoresis were grafted with a polymer coating, as described previously (Hu *et al.* 2002, 2003, 2004*a*,*b*; Wang *et al.* 2005). The monomers used were (poly(ethylene glycol) methyl ether acrylate (MW = 454, 7.7 wt%, PEG acrylate), [2-(methacryloyloxy)ethyl]trimethylammonium chloride (1.92 wt%, MATC) and poly(ethylene glycol) diacrylate (MW = 575, 0.38 wt%, PEG diacrylate).

2.5. Optical delivery system for the pulsed laser beam

The optical set-up for laser-based cell lysis is illustrated in figure 1. A diode-pumped, passively Q-switched Nd : YAG laser (532 nm, 750 ps pulse, vertically polarized beam PowerChip NanoLaser; JDS Uniphase Corp., Milpitas, CA) was steered through a polarizer (LPVIS100 Linear Polarizer; Thorlabs Inc., Newton, NJ) to control the pulse energy. A Keplerian beam expander with a pinhole at the focal point was used to convert the oval beam to a circular Gaussian beam. An iris diaphragm was used to optimize the beam diameter. The beam diameter (7 mm) yielding the lowest energy threshold for optical breakdown in water was used for experiments (Venugopalan *et al.* 2002). A flip-up mirror or coverslip in the beam path (New Focus, San Jose, CA) was used to monitor pulse energy. The beam entered the rear port of a microscope (Eclipse TE300; Nikon Instruments Inc., Melville, NY) where it was reflected upwards to the sample with a dichroic filter reflecting $\lambda < 565$ nm. The laser was focused by an objective (CFI Achromat 60×, N.A. 0.80; Nikon Instruments Inc., Melville, NY) onto the sample. The focal point of the Nd : YAG laser pulse was coincident with the focal plane of the microscope.

For fluorescence measurements, a bandpass filter (FF01-531/22-25; Semrock Inc., Rochester, NY) was inserted into the path of the laser at 8.6°, as shown in figure 1. The beam of the arc lamp was directed onto the bandpass filter so that the arc lamp beam entered the microscope coincident with the laser beam. A neutral density filter (O.D. = 0.3) was inserted immediately in front of the arc lamp to control the light intensity.

2.6. Calculation of effective optical path length

Figure 2*a* shows how the laser beam is focused by the microscope objective into a microfluidic chip. The objective used is corrected for a cover glass thickness of $L_{glass} = 170$ µm with a refractive index of $n_{glass} = 1.515$.

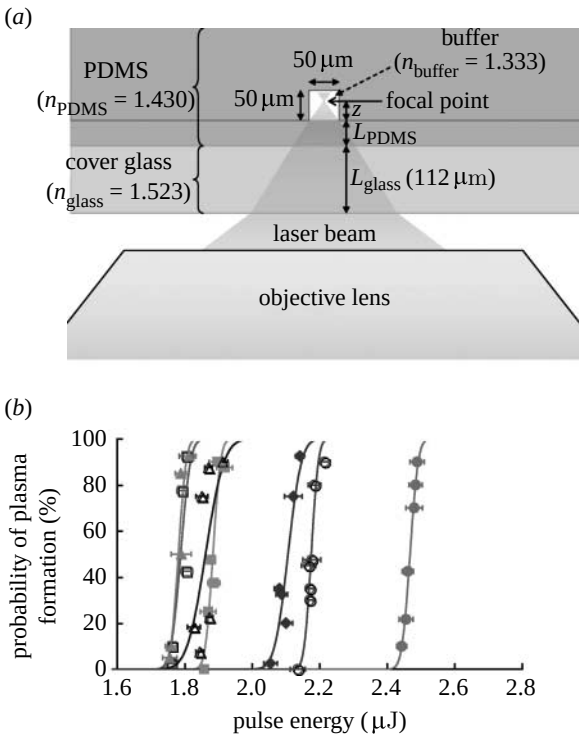

Figure 2. Formation of a plasma within a microchannel. (*a*) Schematic of the objective and microdevice used to determine the probability of plasma formation within a microchannel. (*b*) Curves of the probability of plasma formation with respect to the pulse energy with the laser focused at 6 µm (solid circles), 13 µm (open circles), 19 µm (solid squares), 25 µm (open squares), 31 µm (solid triangles), 38 µm (open triangles) and 44 µm (solid diamonds) above the bottom of the channel were constructed. The PDMS thickness between the coverslip and the channel bottom was 42 µm. The thickness of the coverslip was 112 µm. The lines are the best fits of the data to a Gaussian error function.

In order to quantify the effect introduced by different PDMS thicknesses on the 112 µm cover glass, we introduce an effective optical path length for the focused laser pulse (neglecting the propagation through air),

$$L_{\text{eff}} = n_{\text{glass}} \cdot L_{\text{glass}} + n_{\text{PDMS}} \cdot L_{\text{PDMS}} + n_{\text{buffer}} \cdot z,$$

where L_{glass}, L_{PDMS} and z represent the thickness of cover glass (112 µm), the thickness of the PDMS film and the distance that the laser propagates into the buffer in the channel to the focal point, respectively. The refractive index of the microchannel materials was 1.523 (n_{glass}), 1.430 (n_{PDMS}) and 1.333 (n_{buffer}).

2.7. Measurement of the threshold for plasma formation

When the intensity of the pulsed laser at the focal point reaches a critical value, a plasma is formed and its expansion and collapse produce a cavitation bubble, which is the major mechanism of laser-induced cell lysis. In this section, we investigate the probability of plasma formation as a function of laser pulse energy at different axial positions z (figure 2*a*) inside the microfluidic channel since focusing at different heights (z) changes the effective optical path length of the Nd : YAG laser pulse.

The Nd : YAG laser was focused at varying locations within an ECB-filled microchannel (ECB buffer: 135 mM NaCl, 5 mM KCl, 10 mM HEPES, 1 mM $MgCl_2$ and 1 mM $CaCl_2$ (pH 7.4)). When the intensity of the pulsed laser was sufficient to produce a plasma, luminescence was observed at visible wavelengths using a CCD camera equipped with a notch filter at 532 nm (NF02-532S-25 StopLine Notch Filter; Semrock Inc., Rochester, NY) to reject the laser light. The incidence of plasma formation for at least 10 pulses was recorded for each laser energy setting. The actual pulse energy each time the laser was fired was also measured. Six or seven different laser energy settings were used for each different focal plane of the laser. The probability of plasma formation [$P(E)$] for each different focal plane was plotted and fitted with a Gaussian error function (Vogel *et al.* 1996*b*), which is given by

$$P(E) = \frac{1}{2}\left[1 + \text{erf}\left(\frac{E - E_{\text{T}}}{\sqrt{2\sigma}}\right)\right], \qquad (2.1)$$

where E is the pulse energy, σ is a fitting parameter that characterizes the sharpness of the curve and E_{T} is the threshold energy for plasma formation or the energy for which a plasma is formed 50% of the time.

2.8. Fluorescence microscopy

Images of cells were captured using a monochrome CCD camera (Photometrics CoolSNAP *fx*; Roper Scientific Inc., Tucson, AZ) through a bright-field objective lens (CFI Achromat 60×, N.A. 0.80, W.D. 0.3 mm; Nikon Instruments Inc., Melville, NY) and a Nikon standard fluorescein filter set (excitation, 465–495 nm; dichroic, 505 nm; emission, 515–555 nm) in an inverted fluorescence microscope (Eclipse TE300; Nikon Instruments Inc., Melville, NY). MetaFluor software (Molecular Devices Corp., Downingtown, PA) was used to collect the images.

2.9. Electrophoresis of the contents of a cell lysed in a microchannel

Separation of a cell's contents was performed on the microchips described above with a cross-channel geometry. BA/F3 cells loaded with Oregon Green and fluorescein (3×10^5 to 10×10^5 cells ml^{-1}) were added into reservoir 1 of the microchip (see figure 5*a*). All other reservoirs and the channels were filled with the isotonic buffer. The cells were then moved by hydrodynamic flow from reservoirs 1 to 3. An intact single cell was loaded into the channel leading to reservoir 4 by pressure-driven flow. The fluid levels in the reservoir were manually adjusted to achieve this. The target single cell was moved 10 mm downstream from the intersection and fluid flow was terminated permitting the cell to settle to the bottom of the microchannel. To lyse the cell, the cell was centred over the path of the focused laser pulse. The focal point of the laser was 6 µm above the channel floor. A single focused pulse (4.2 µJ) was delivered through the bottom of the channel (42 µm thick PDMS on No. 0 cover glass) and electrophoresis was immediately initiated. For electrophoretic separation of the lysed

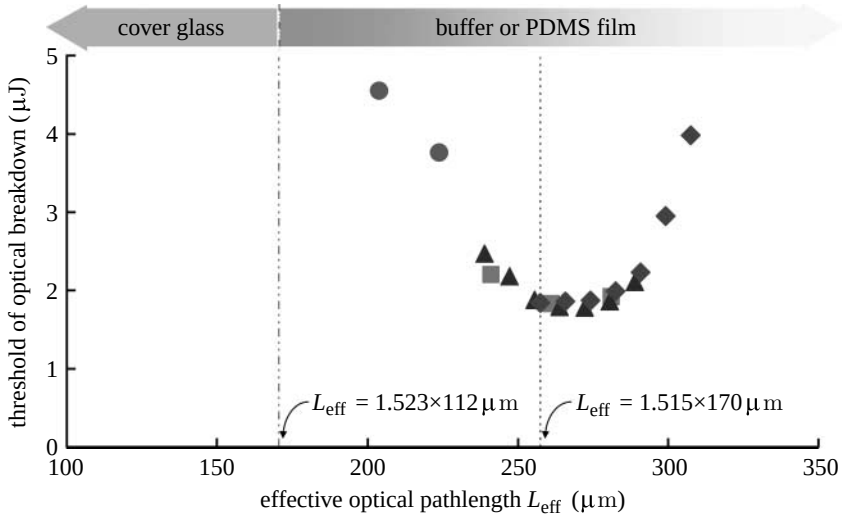

Figure 3. Dependence of the threshold for plasma formation on L_{eff}. The threshold of optical breakdown in an ECB-filled microchannel was measured at different heights above the bottom of the channel. The floor of the channel was a coverslip coated with a PDMS film of varying thickness (circles, 0 μm, (bare glass); squares, 40 μm; triangles, 42 μm; diamonds, 55 μm). L_{eff} was calculated for the different focal points of the beam as well as the PDMS thickness and then plotted against the threshold for plasma formation.

cell's contents, 500 V was applied to reservoirs 1–3 and 4 was held at ground. Fluorescence was detected 3 mm from the point of lysis using a customized LIF module with excitation a 473 nm (Lasermate Group Inc., Pomona, CA) and emission at 535 nm (HQ 535/50M; Chroma Technology Corp., Rockingham, VT). Data were acquired at 1 kHz with custom software written in TestPoint (Keithley Instruments, Inc., Cleveland, OH). To establish the migration times of Oregon Green and fluorescein, electrophoresis of standards was performed on a microchip with a cross-channel geometry, as described previously (Hu *et al.* 2003, 2004*a*).

3. RESULTS AND DISCUSSION

3.1. Plasma formation at different depths within a microchannel

When a pulsed laser beam is focused to a sufficiently small diameter, a localized plasma can be created, which in turn produces an outwardly propagating shock wave and an expanding cavitation bubble (Vogel *et al.* 1996*a*; Noack *et al.* 1998). The cavitation bubble and induced shear stresses can result in the lysis of cells in proximity to the focal point of the laser beam (Rau *et al.* 2006; Hellman *et al.* 2008). With a polymer microdevice, the laser beam must pass through a portion of the polymer that can alter the probability of forming a plasma within the channel. To determine the probability of plasma formation in a polymer microchannel, the beam of a pulsed laser was focused within a microchannel bounded on all sides by PDMS (figure 2*a*). The base of the channel through which the beam transited was composed of a cover glass with a 42 μm layer of PDMS. For the most efficient cell lysis, it may also be desirable to move the focal point of the laser to different locations within the microchannel. Therefore, the focal plane of the laser beam was placed at different locations within the channel and the threshold energy for plasma formation was measured (figure 2*b*). The threshold energy for plasma formation was 2.5, 2.2, 1.9, 1.8, 1.8, 1.9 and 2.1 μJ at 6, 13, 19, 25, 31, 38 and 44 μm, respectively, from the bottom of the channel. When a very thin layer of PDMS was used as the base of the channel, the pulsed beam could be focused at any location in the channel with minimal changes in the threshold energy for plasma formation.

To determine how the thickness of the PDMS layer influenced the ability to form a plasma within the channel, the probability of plasma formation at varying channel locations was also determined using devices with PDMS base thicknesses of 0, 40 and 55 μm. The threshold energy for plasma formation was plotted against the effective optical path length (L_{eff}), the distance between the bottom of the coverslip and the laser focal point corrected for the refractive indices of the different materials (figure 3). The lowest thresholds (1.8–1.9 μJ) were achieved for 255 μm $< L_{eff} <$ 280 μm for all tested thicknesses of the PDMS base. This was also the case for a coverslip without a PDMS coating. This optimal L_{eff} range for plasma formation matches that recommended by the objective manufacturer ($L_{eff} = 1.515 \times 170$ μm $= 258$ μm), suggesting that the thin PDMS layer does not introduce substantial aberrations in focusing the laser light. For L_{eff} values smaller than 235 μm or greater than 295 μm, the threshold energy for plasma formation rapidly escalated to values greater than 2.5 μJ. At these L_{eff} values, the specifications of the objective were exceeded and introduced aberrations that increased the required laser energies. Therefore, for a 50 μm microchannel, the range of PDMS base thicknesses that permitted plasma formation at low energies (less than 2.5 μJ) in all regions of the channel was 40–45 μm. For this objective and others, the threshold for optical breakdown along with the effective optical path length forms a guideline for the optimal microfluidic dimensions, particularly the thickness of the lower polymer layer.

3.2. Influence of laser-generated plasma on polymer channel integrity

When a focused laser beam is delivered within a microfluidic device for plasma formation, the processes associated with the plasma expansion and dissipation (i.e. shock wave emission, cavitation bubble expansion and collapse) may have destructive effects on nearby channel walls (Hellman *et al.* 2007; Quinto-Su *et al.* 2008). To determine whether the plasma generated within the channel could damage the soft PDMS walls, the channels were imaged before and after the formation of a plasma using a laser pulse energy (4.8 µJ) that was two times or greater than the threshold for plasma formation. The laser beam was focused 6, 13, 19, 25, 31, 38 and 44 µm from the bottom of the channel. Even after repeated pulses ($n=10$), no damage to any portion of the channel was observed. Thus, even when a plasma is formed as close as 6 µm from the PDMS, the PDMS remains intact. This is most likely due to the flexing of PDMS that can occur on rapid time scales (Hellman *et al.* 2007; Quinto-Su *et al.* 2008). The PDMS could be damaged when the laser beam (1.6× threshold) was focused at the interface of the PDMS:buffer solution at either the top or the bottom of the channel. However, even in this instance only a small divot less than 1 µm in diameter was formed in the PDMS. The channel itself remained intact and no separation/delamination of the PDMS layers forming the top and the bottom of the channel was ever observed. Thus, the laser could be focused to generate a plasma at any location in the channel without compromising the integrity of the microdevice.

3.3. Spatial restriction of cell lysis in a microchannel by a pulsed laser beam

Cells within a microchannel can be either lysed or porated by a pulsed laser beam. Soughayer *et al.* used a Nd : YAG laser (532 nm) with a 5 ns pulse duration to porate cells in a glass microchannel (Soughayer *et al.* 2000). These investigators reported that cells within 50 µm of the focused beam were lysed while those as far away as 200 µm were porated or reversibly permeabilized. The effects of plasma formation were felt by the cells at long distances from the beam location in the glass microchannel. Under these conditions, the cells flowing through the microchannel must be widely spaced to avoid perturbation of adjacent non-targeted cells. Consequently, single-cell interrogation at high throughput would be difficult with the 5 ns pulse in a glass microdevice. Quinto-Su *et al.* used a 500 ps pulse focused directly within a cell-for-cell lysis in a PDMS–glass hybrid microchannel (Quinto-Su *et al.* 2008). These data, along with time lapse imaging demonstrating flexing of the PDMS in response to the forces generated by the laser, suggest that the effects of the pulsed beam may be quite localized in the PDMS channels. To determine the allowable distances between the laser pulse and the cell in a device composed entirely of PDMS, the focal point of the laser was moved axially (z) to different locations within a channel and with respect to a cell. The cells were loaded with the viability dye Oregon Green, then placed into a microchannel and permitted to settle to the bottom of the channel. The laser focal point was placed 6, 13, 25 and 38 µm from the bottom of the channel directly over the cell. Since the cells have a diameter of 15 µm, the 6 and 13 µm locations probably placed the beam focal point within the cell. The laser pulse energy was also varied (0.8–2.2× threshold) for each focal point within the microchannel. The cell was examined by transmitted light and fluorescence microscopy before and after the delivery of the single pulse to examine the cellular morphology and determine whether the Oregon Green was lost from the cell. When the beam was near the centre of the cell (6 µm from the channel bottom), all tested energies were effective in lysing the cell as evidenced by an altered cellular morphology and loss of the intracellular Oregon Green (figure 4). As the beam height was increased to 13 µm, which was probably just inside the cell's plasma membrane, 90% of the cells were lysed at energies of 1.8× threshold but only 50% at energies of 0.8× threshold. Placing the beam 25 µm above the channel bottom or approximately 10 µm above the cell rarely resulted in cell lysis. No cell lysis was observed at beam heights greater than 25 µm above the channel bottom. For a pulse duration of 750 ps in a PDMS channel, the laser microbeam must be within 6 µm from the cell centre to effect cell lysis. Thus, the effects of the pulsed microbeam were spatially restricted to a very small volume in these PDMS microchannels. This was most likely due to the flexing of the PDMS observed by Quinto-Su *et al.* (2008), which attenuated the forces generated by the cavitation bubble dynamics. Single-cell interrogation or lysis using a pulsed microbeam should be easily attained in a PDMS microchannel when the cells are spaced by as little as a few micrometres.

3.4. Laser-based cell lysis followed by electrophoresis of the cellular contents

The spatially restricted actions of the 750 ps laser pulse and the time scale on which the plasma forms suggested that the contents of the cell may remain sufficiently concentrated for immediate electrophoretic separation following lysis. A cell containing Oregon Green and fluorescein was loaded into a microchannel, permitted to settle to the channel bottom and then washed with an isotonic buffer solution (figure 5*a*). The cell was lysed by application of a single laser pulse (4.2 µJ) focused within the cell (6 µm from the bottom of the channel). A voltage was applied across the channel and fluorescence detected 3 mm from the lysed cell. Two peaks were observed with migration times similar to those of standards of fluorescein and Oregon Green ($n=3$ cells; figure 5*b*,*c*). The resolution and efficiency of the electrophoretic separation in these experiments were calculated based on the migration times and peak widths (Harvey 2000; Hu *et al.* 2003). The fluorophores were separated with a resolution of 1.1 ± 0.4 (field strength, 175 V cm^{-1}) in the isotonic, mannitol-containing buffer. The theoretical plates were 1200 ± 600 cm^{-1} for fluorescein and 900 ± 700 cm^{-1} for

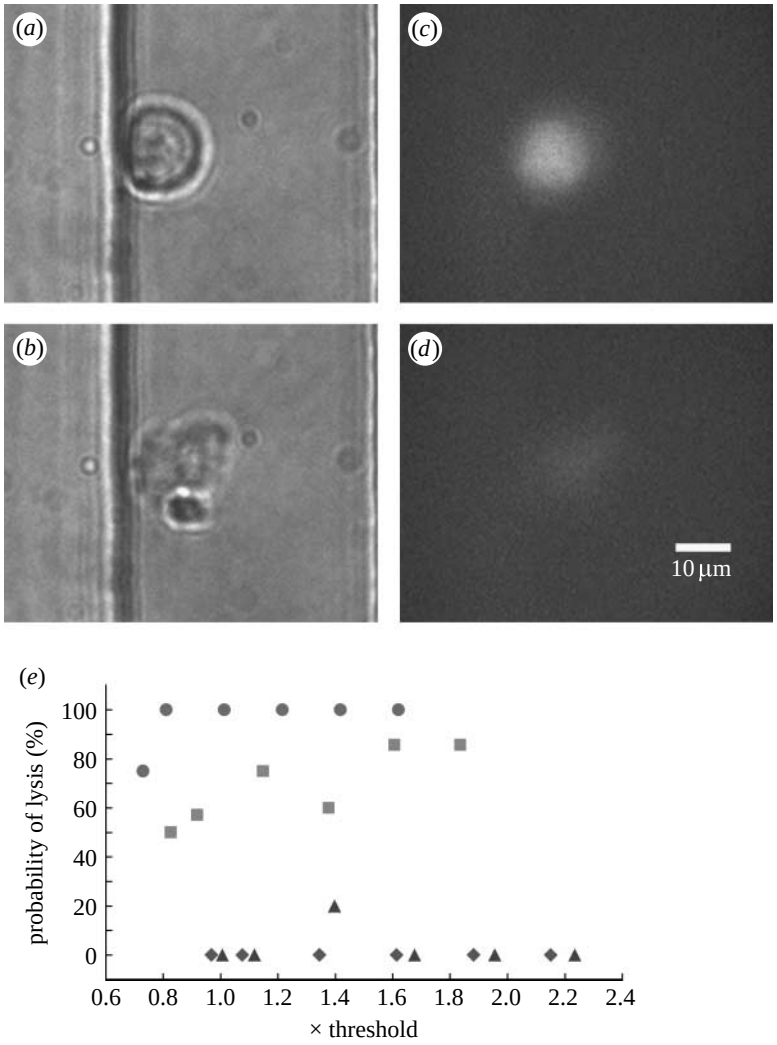

Figure 4. Cell lysis in a microchannel with a pulsed laser beam. (*a*,*b*) Transmitted light and (*c*,*d*) fluorescence images of a cell (*a*,*c*) before and (*b*,*d*) after cell lysis. The focal point of the laser pulse (4.2 µJ) was 6 µm above the bottom of the microchannel. (*e*) Graphs of the pulse energy versus percentage of cells lysed with respect to laser focus location *z* (circles, 6 µm; squares, 13 µm; triangles, 25 µm; diamonds, 38 µm), which was measured relative to the bottom of the PDMS microchannel. A minimum of five cells were targeted for each energy and each laser beam location.

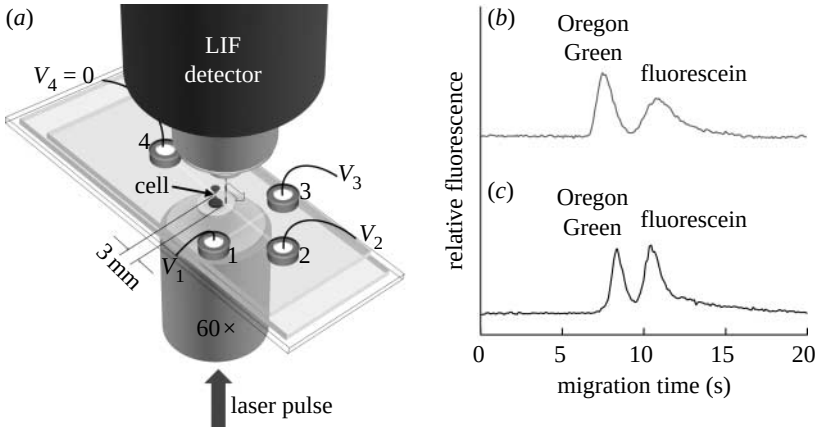

Figure 5. Electrophoretic separation of the contents of a single cell in a microchannel. (*a*) Schematic of the microfluidic chip for separation of the cellular contents. (*b*) Electropherogram of fluorescein (2 µM) and Oregon Green (1 µM) standards in the isotonic buffer in the surface-modified PDMS microchannel. The migration time of fluorescein and Oregon Green standards was 11 and 8 s, respectively. (*c*) Electropherogram of the contents from a BA/F3 cell, which was incubated with the esterified analogues of fluorescein and Oregon Green. The fluorescence of the peaks representing fluorescein and Oregon Green was equivalent to 5.4 and 1.4 µM, respectively. The migration time of fluorescein and Oregon Green obtained from the cell was 11 and 9 s, respectively.

Oregon Green, which were similar to those obtained when fluorescein and Oregon Green standards were separated in the isotonic, mannitol solution in a microfluidic channel. These separation properties were lower in quality than those obtained for standards in an alternative electrophoretic buffer (Tris, 25 mM; glycine buffer, 192 mM (pH 8.4), data not shown; Hu *et al.* 2003, 2004*a*). These results suggested that the isotonic, mannitol buffer while maintaining the proper cellular osmolarity was not an optimal electrophoretic buffer. The intracellular concentration of the analytes was measured by comparing the peak areas of the cell-derived analyte peaks with those of standards with known injection volumes. Assuming a cell volume of 1 pl, the intracellular concentration was 3.0 ± 2.1 μM for fluorescein and 1.1 ± 0.9 μM for Oregon Green. These concentrations are in the expected range for the fluorophore loading conditions, although we cannot exclude partial degradation of the fluorophore by the beam used for cell lysis (Sims *et al.* 1998).

4. CONCLUSIONS

In this work, we have demonstrated cell lysis by a pulsed, focused laser beam followed by electrophoretic separation of two intracellular analytes. Since the laser beam produces a very small zone of lysis and the effects of the pulsed beam are extremely brief, the cells can be targeted for lysis with high precision in both space and time. Thus, it may be possible to selectively lyse closely spaced cells in a flowing stream within a microfluidic device. For the measurement of intracellular analytes with concentrations changing on time scales of milliseconds to seconds, the focused, pulsed beam may be particularly attractive since the fast lysis times (approx. microseconds) have the potential to rapidly terminate cellular reactions. While the feasibility of laser-based cell lysis combined with electrophoretic separation in a microfluidic device has been demonstrated, optimization of the electrophoretic buffer remains a challenge, particularly when the cell must be maintained in a physiological buffer until the moment of lysis.

This research was supported by a grant from the National Institutes of Health (EB4436). The authors thank Ruisheng Chang for silicon mould fabrication, Lavanya Rau and Paul Marc for design and assembly of the LIF detection system and Ayla Munawar for making the PDMS-coated coverslips.

REFERENCES

Berridge, M. J. 1993 Inositol trisphosphate and calcium signaling. *Nature* **361**, 315–325. (doi:10.1038/361315a0)

Braschler, T., Johann, R., Heule, M., Metref, L. & Renaud, P. 2005 Gentle cell trapping and release on a microfluidic chip by *in situ* alginate hydrogel formation. *Lab Chip* **5**, 553–559. (doi:10.1039/b417604a)

Di Carlo, D. & Lee, L. P. 2006 Dynamic single-cell analysis for quantitative biology. *Anal. Chem.* **78**, 7918–7925.

Dovichi, N. J. & Hu, S. 2003 Chemical cytometry. *Curr. Opin. Chem. Biol.* **7**, 603–608. (doi:10.1016/j.cbpa.2003.08.012)

Evander, M., Johansson, L., Lilliehorn, T., Piskur, J., Lindvall, M., Johansson, S., Almqvist, M., Laurell, T. & Nilsson, J. 2007 Noninvasive acoustic cell trapping in a microfluidic perfusion system for online bioassays. *Anal. Chem.* **79**, 2984–2991. (doi:10.1021/ac061576v)

Gao, J., Yin, X. F. & Fang, Z. L. 2004 Integration of single cell injection, cell lysis, separation and detection of intracellular constituents on a microfluidic chip. *Lab Chip* **4**, 47–52. (doi:10.1039/b310552k)

Harvey, D. 2000 *Modern analytical chemistry*. New York, NY: The McGraw-Hill.

He, M. Y., Edgar, J. S., Jeffries, G. D. M., Lorenz, R. M., Shelby, J. P. & Chiu, D. T. 2005 Selective encapsulation of single cells and subcellular organelles into picoliter- and femtoliter-volume droplets. *Anal. Chem.* **77**, 1539–1544. (doi:10.1021/ac0480850)

Hellman, A. N., Rau, K. R., Yoon, H. H., Bae, S., Palmer, J. F., Phillips, K. S., Allbritton, N. L. & Venugopalan, V. 2007 Laser-induced mixing in microfluidic channels. *Anal. Chem.* **79**, 4484–4492. (doi:10.1021/ac070081i)

Hellman, A. N., Rau, K. R., Yoon, H. H. & Venugopalan, V. 2008 Biophysical response to pulsed laser microbeam-induced cell lysis and molecular delivery. *J. Biophoton.* **1**, 24–35. (doi:10.1002/jbio.200710010)

Hellmich, W., Pelargus, C., Leffhalm, K., Ros, A. & Anselmetti, D. 2005 Single cell manipulation, analytics, and label-free protein detection in microfluidic devices for systems nanobiology. *Electrophoresis* **26**, 3689–3696. (doi:10.1002/elps.200500185)

Hellmich, W., Greif, D., Pelargus, C., Anselmetti, D. & Ros, A. 2006 Improved native UV laser induced fluorescence detection for single cell analysis in poly(dimethylsiloxane) microfluidic devices. *J. Chromatogr. A* **1130**, 195–200. (doi:10.1016/j.chroma.2006.06.008)

Hu, S. W., Ren, X. Q., Bachman, M., Sims, C. E., Li, G. P. & Allbritton, N. L. 2002 Surface modification of poly(dimethylsiloxane) microfluidic devices by ultraviolet polymer grafting. *Anal. Chem.* **74**, 4117–4123. (doi:10.1021/ac025700w)

Hu, S. W., Ren, X. Q., Bachman, M., Sims, C. E., Li, G. P. & Allbritton, N. L. 2003 Cross-linked coatings for electrophoretic separations in poly(dimethylsiloxane) microchannels. *Electrophoresis* **24**, 3679–3688. (doi:10.1002/elps.200305592)

Hu, S. W., Ren, X. Q., Bachman, M., Sims, C. E., Li, G. P. & Allbritton, N. L. 2004*a* Surface-directed, graft polymerization within microfluidic channels. *Anal. Chem.* **76**, 1865–1870. (doi:10.1021/ac049937z)

Hu, S. W., Ren, X. Q., Bachman, M., Sims, C. E., Li, G. P. & Allbritton, N. L. 2004*b* Tailoring the surface properties of poly(dimethylsiloxane) microfluidic devices. *Langmuir* **20**, 5569–5574. (doi:10.1021/la049974l)

Huang, B., Wu, H. K., Bhaya, D., Grossman, A., Granier, S., Kobilka, B. K. & Zare, R. N. 2007 Counting low-copy number proteins in a single cell. *Science* **315**, 81–84. (doi:10.1126/science.1133992)

Johann, R. M. 2006 Cell trapping in microfluidic chips. *Anal. Bioanal. Chem.* **385**, 408–412. (doi:10.1007/s00216-006-0369-6)

Kleparnik, K. & Horky, M. 2003 Detection of DNA fragmentation in a single apoptotic cardiomyocyte by electrophoresis on a microfluidic device. *Electrophoresis* **24**, 3778–3783. (doi:10.1002/elps.200305667)

Lacroix, M., Poinsot, V., Fournier, C. & Couderc, F. 2005 Laser-induced fluorescence detection schemes for the analysis of proteins and peptides using capillary electrophoresis. *Electrophoresis* **26**, 2608–2621. (doi:10.1002/elps.200410414)

Li, H. N., Sims, C. E., Wu, H. Y. & Allbritton, N. L. 2001 Spatial control of cellular measurements with the laser micropipet. *Anal. Chem.* **73**, 4625–4631. (doi:10.1021/ac0105235)

Li, P. C. H. & Harrison, D. J. 1997 Transport, manipulation, and reaction of biological cells on-chip using electrokinetic effects. *Anal. Chem.* **69**, 1564–1568. (doi:10.1021/ac9606564)

Lin, Y. W., Chiu, T. C. & Chang, H. T. 2003 Laser-induced fluorescence technique for DNA and proteins separated by capillary electrophoresis. *J. Chromatogr. B* **793**, 37–48. (doi:10.1016/S1570-0232(03)00363-5)

Lu, H., Schmidt, M. A. & Jensen, K. F. 2005 A microfluidic electroporation device for cell lysis. *Lab Chip* **5**, 23–29. (doi:10.1039/b406205a)

Martin, R. S., Root, P. D. & Spence, D. M. 2006 Microfluidic technologies as platforms for performing quantitative cellular analyses in an in vitro environment. *Analyst* **131**, 1197–1206. (doi:10.1039/b611041j)

McClain, M. A., Culbertson, C. T., Jacobson, S. C., Allbritton, N. L., Sims, C. E. & Ramsey, J. M. 2003 Microfluidic devices for the high-throughput chemical analysis of cells. *Anal. Chem.* **75**, 5646–5655. (doi:10.1021/ac0346510)

Meredith, G. D., Sims, C. E., Soughayer, J. S. & Allbritton, N. L. 2000 Measurement of kinase activation in single mammalian cells. *Nat. Biotechnol.* **18**, 309–312. (doi:10.1038/73760)

Munce, N. R., Li, J. Z., Herman, P. R. & Lilge, L. 2004 Microfabricated system for parallel single-cell capillary electrophoresis. *Anal. Chem.* **76**, 4983–4989. (doi:10.1021/ac0496906)

Noack, J., Hammer, D. X., Noojin, G. D., Rockwell, B. A. & Vogel, A. 1998 Influence of pulse duration on mechanical effects after laser-induced breakdown in water. *J. Appl. Phys.* **83**, 7488–7495. (doi:10.1063/1.367512)

Paez, X. & Hernandez, L. 2001 Biomedical applications of capillary electrophoresis with laser-induced fluorescence detection. *Biopharm. Drug Dispos.* **22**, 273–289. (doi:10.1002/bdd.277)

Price, A. K. & Culbertson, C. T. 2007 Chemical analysis of single mammalian cells with microfluidics. Strategies for culturing, sorting, trapping, and lysing cells and separating their contents on chips. *Anal. Chem.* **79**, 2614–2621.

Quinto-Su, P. A., Lai, H. H., Yoon, H. H., Sims, C. E., Allbritton, N. L. & Venugopalan, V. 2008 Examination of laser microbeam cell lysis in a PDMS microfluidic channel using time-resolved imaging. *Lab Chip* **8**, 408–414. (doi:10.1039/b715708h)

Rau, K. R., Guerra, A., Vogel, A. & Venugopalan, V. 2004 Investigation of laser-induced cell lysis using time-resolved imaging. *Appl. Phys. Lett.* **84**, 2940–2942. (doi:10.1063/1.1705728)

Rau, K. R., Quinto-Su, P. A., Hellman, A. N. & Venugopalan, V. 2006 Pulsed laser microbeam-induced cell lysis: Time-resolved imaging and analysis of hydrodynamic effects. *Biophys. J.* **91**, 317–329. (doi:10.1529/biophysj.105.079921)

Ren, X. Q., Bachman, M., Sims, C., Li, G. P. & Allbritton, N. 2001 Electroosmotic properties of microfluidic channels composed of poly(dimethylsiloxane). *J. Chromatogr. B* **762**, 117–125. (doi:10.1016/S0378-4347(01)00327-9)

Ros, A., Hellmich, W., Regtmeier, J., Duong, T. T. & Anselmetti, D. 2006 Bioanalysis in structured microfluidic systems. *Electrophoresis* **27**, 2651–2658. (doi:10.1002/elps.200500923)

Sims, C. E. & Allbritton, N. L. 2007 Analysis of single mammalian cells on-chip. *Lab Chip* **7**, 423–440. (doi:10.1039/b615235j)

Sims, C. E., Meredith, G. D., Krasieva, T. B., Berns, M. W., Tromberg, B. J. & Allbritton, N. L. 1998 Laser–micropipet combination for single-cell analysis. *Anal. Chem.* **70**, 4570–4577. (doi:10.1021/ac9802269)

Soughayer, J. S., Krasieva, T., Jacobson, S. C., Ramsey, J. M., Tromberg, B. J. & Allbritton, N. L. 2000 Characterization of cellular optoporation with distance. *Anal. Chem.* **72**, 1342–1347. (doi:10.1021/ac990982u)

Tan, Y. C., Hettiarachchi, K., Siu, M., Pan, Y. R. & Lee, A. P. 2006 Controlled microfluidic encapsulation of cells, proteins, and microbeads in lipid vesicles. *J. Am. Chem. Soc.* **128**, 5656–5658. (doi:10.1021/ja056641h)

Venugopalan, V., Guerra, A., Nahen, K. & Vogel, A. 2002 Role of laser-induced plasma formation in pulsed cellular microsurgery and micromanipulation. *Phys. Rev. Lett.* **88**, 078 103. (doi:10.1103/PhysRevLett.88.078103)

Vogel, A., Busch, S. & Parlitz, U. 1996*a* Shock wave emission and cavitation bubble generation by picosecond and nanosecond optical breakdown in water. *J. Acoust. Soc. Am.* **100**, 148–165. (doi:10.1121/1.415878)

Vogel, A., Nahen, K., Theisen, D. & Noack, J. 1996*b* Plasma formation in water by picosecond and nanosecond Nd:YAC laser pulses. 1. Optical breakdown at threshold and superthreshold irradiance. *IEEE J. Sel. Top. Quantum Electron.* **2**, 847–860. (doi:10.1109/2944.577307)

Wang, Y. L., Lai, H.-H., Bachman, M., Sims, C. E., Li, G. P. & Allbritton, N. L. 2005 Covalent micropatterning of poly(dimethylsiloxane) by photografting through a mask. *Anal. Chem.* **77**, 7539–7546. (doi:10.1021/ac0509915)

Wang, Y. L., Sims, C. E., Marc, P., Bachman, M., Li, G. P. & Allbritton, N. L. 2006 Micropatterning of living cells on a heterogeneously wetted surface. *Langmuir* **22**, 8257–8262. (doi:10.1021/la061602k)

Wang, L., Flanagan, L. A., Jeon, N. L., Monuki, E. & Lee, A. P. 2007 Dielectrophoresis switching with vertical sidewall electrodes for microfluidic flow cytometry. *Lab Chip* **7**, 1114–1120. (doi:10.1039/b705386j)

Waters, L. C., Jacobson, S. C., Kroutchinina, N., Khandurina, J., Foote, R. S. & Ramsey, J. M. 1998 Microchip device for cell lysis, multiplex PCR amplification, and electrophoretic sizing. *Anal. Chem.* **70**, 158–162. (doi:10.1021/ac970642d)

Wood, D. K., Oh, S. H., Lee, S. H., Soh, H. T. & Cleland, A. N. 2005 High-bandwidth radio frequency Coulter counter. *Appl. Phys. Lett.* **87**, 184 106. (doi:10.1063/1.2125111)

Woods, L. A., Roddy, T. P. & Ewing, A. G. 2004 Capillary electrophoresis of single mammalian cells. *Electrophoresis* **25**, 1181–1187. (doi:10.1002/elps.200405842)

Wu, H. K., Wheeler, A. & Zare, R. N. 2004 Chemical cytometry on a picoliter-scale integrated microfluidic chip. *Proc. Natl Acad. Sci. USA* **101**, 12 809–12 813. (doi:10.1073/pnas.0405299101)

Zhang, X., Stuart, J. N. & Sweedler, J. V. 2002 Capillary electrophoresis with wavelength-resolved laser-induced fluorescence detection. *Anal. Bioanal. Chem.* **373**, 332–343. (doi:10.1007/s00216-002-1288-9)